SIZE EFFECTS OF DISCOIDAL PLGA NANOCONSTRUCTS IN PICKERING EMULSION STABILIZATION

Alexander B. Cook*, Michele Schlich, Purnima N. Manghnani,

Thomas L. Moore, Paolo Decuzzi, AnnaLisa Palange

Laboratory of Nanotechnology for Precision Medicine

Istituto Italiano di Tecnologia

Via Morego 30, 16163, Genova, Italy

Corresponding author: Alexander B. Cook a.b.cook@tue.nl

TOC:

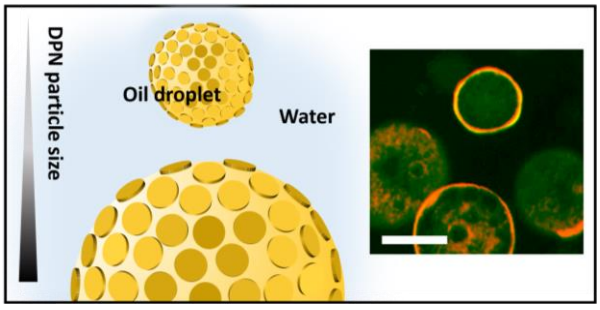

Keywords: anisotropic particles, biodegradable, emulsion stabilization, discoidal particles, formulations

ABSTRACT

Solid particle stabilised emulsions, using unique shape defined particles, are receiving increasing research interest due to ease of formulation and interesting physiochemical characteristics. There is, however, a need to systematically investigate the effect of anisotropic discoidal microparticles, realised with top-down fabrication approaches, in emulsion stabilization. Here, the effect of poly(D,L-lactide-*co*-glycolide) (PLGA) discoidal polymeric nanoconstruct (DPN) size on the formation and stability of oil-in-water emulsions is studied. Particles with a diameter of 1, 2, and 5 μm are fabricated with a lithographic templating technique, and used to stabilise medium chain triglyceride (MCT) oil emulsions. Three phase contact angles decreased from 85° ± 7° to 68° ± 12° moving from 1 to 5 μm DPN stabilised emulsions, showing a particle 'hydrophilicity' increase with size. Microscopy imaging showed that the mean droplet diameter and dispersity increased with particle size, and that DPNs were present at the oil-water interface. DPN based emulsions were stable for about 24 hours or less in the case of 1 and 2 μm DPNs. Emulsion stability was shorter than 12 hours in case of 5 μm DPNs. Finally, calculations of DPN detachment free energies ΔG_{dw} and excess surface coverages C_{excess} demonstrated that, despite the significantly high adhesion energy of the discoidal DPN, emulsion stability was mostly affected by gravitational forces for DPN sizes above 2 μm. The use of PLGA and MCT oil in this study is relevant for future use of Pickering emulsions in pharmaceutical and drug delivery applications.

INTRODUCTION

Stable emulsions are vital for many different applications from food, cosmetics, consumer goods, pharmaceuticals, and biotechnology.[1–4] Typically, surfactants are needed to stabilise the high interfacial area of the normally thermodynamically unstable immiscible liquid systems. Emulsions stabilised by the presence of colloidal particles adsorbed at the liquid-liquid interface are commonly known as Pickering emulsions.[5–8] Interest in the use of nanoparticles and microparticles to stabilise the interface has increased in recent decades due to the increasing ability to synthesise new and more complex particles with different compositions, size and shapes, surface properties, and mechanical deformability. Pickering emulsions allow incorporation of additional functionality, such as stimuli responsiveness,[9–12] through rational design of particle properties, and can also be used to fabricate various capsules and colloidosomes for drug delivery and use as nanoreactors.[13–16]

Particle stabilised emulsions are important industrially and have found application in a wide range of fields. In particular, food, cosmetics, and pharmaceutical applications of Pickering emulsions are common. Biocompatibility and/or biodegradablility of the particles used is therefore important. In the food industry, there are many examples of protein particle stabilised emulsions. Protein particles can be prepared from natural sources such as soy, whey, ferritin, pea, beta-lactoglobulin, through different techniques including precipitation, heat treatment, mechanical homogenization.[1,17] Liu *et al*., investigated the encapsulation of β-carotene in the oil phase of Pickering emulsions stabilised with protein particles derived from soy.[18] They characterized the emulsion droplets in the range of tens of micrometers, the active ingredient was protected from degradation in the oil phase, and there was a sustained release of the active ingredient during an *in vitro* digestion assay. Chitosan and chitosan coated silica particles are commonly used to stabilise biphasic systems in the food and cosmetics industries.[19,20] As therapeutic formulations, emulsions stabilised by silica nanoparticles, polysaccharide particles, synthetic polymer particles, and chitosan, amongst other examples, are also used.[1,21] Pickering emulsions in pharmaceutics are used for topical, intramuscular, subcutanaeous, and oral applications, with a smaller proportion for intravenous administration (mainly due to the large size of some particle stabilisers making them

unsuitable for intravenous injections). Particles have been shown to be an effective method to modulate drug release kinetics from oil phases.[22] Chevalier and colleagues, reported a silica particle stabilised emulsion system for the topical delivery of lipophilic drugs.[23] In a skin permeation model the Pickering emulsion showed accumulation in the stratum corneum, with large amounts of the active ingredient remaining in this tissue compartment. The authors hypothesized that the formulation could be used to target the stratum corneum and act as a local depot for sustain release into deeper layers of the skin. Cellulose particles have been used as stabilisers in antimicrobial formulations, where the emulsions showed better antimicrobial activity compared to the non emulsified essential oil.[24] When it comes to particles consisting of synthetic polymers, there are fewer options available. PLGA particles are beginning to be investigated.[25,26] Researchers from the Universite Paris-Saclay, have investigated use of PLGA nanoparticles as stabilisers for formulations of chemotherapeutic Oxaliplatin with an oil phase of Lipidol.[27] The emulsion was injected into the hepatic artery of rabbits bearing VX2 liver tumours. Huang and co-workers also investigated more fundamental aspects of PLGA nanoparticle stabilised emulsions of the oil Miglyol, and found that particles benefiting from poly(vinyl alcohol) (PVA) polymer chain steric stabilisation were able to form more uniform oil droplets with better particle adsorption at the interface.[28] While these examples show a number of consumer and pharmaceutical applications of Pickering emulsions, PLGA is one of the few options for biodegradable particle stabilisers.

As the ability of researchers to fabricate particles of varying size, shape, and mechanical properties increases so does the number of studies using these particles in Pickering emulsions.[6,29,30] Variation of particle stiffness can affect emulsion stability, with soft microgels being shown to adopt deformed ‘fried-egg’ like morphologies at liquid interfaces.[31–33] The effect of spherical particle size on emulsion stability has been investigated by Binks *et al*., and Destribats *et al*., who found that with increasing particle size the formed emulsions transitioned from dispersed drops to larger drop sizes and higher flocculation.[34,35] Anisotropic particle stabilisers, can have different interfacial activity compared to spherical particles, and therefore can affect emulsion droplet size and stability. Laponite clay platelets have been the most studied of disk shaped particle morphologies.[36–38] Other disk shaped particles include: zirconium phosphate plate-like crystals,[39] 2D poly(lactide) polymer platelets,[40] and hexagonal gibbsite platelets.[41] Madivala *et al*. prepared

elliptical polystyrene particles and investigated the stability of Pickering emulsions compared to spherical particles.[42] The anisotropic elliptical particles were able to stabilise emulsions more effectively and to an increasing extend with higher aspect ratio rods. Similarly, cellulose nanorods[43,44] and hematite ellipsoidal microparticles,[45] have been shown to effectively stabilise water-in-water and oil-in-water emulsions with the authors hypothesizing droplet stability being due to efficient side by side ellipsoid packing arrangements. Although these cases highlight recent advances in anisotropic particle Pickering emulsions, there are still limited examples as the fabrication of complex particle shapes and morphologies remains challenging.

The Decuzzi group has expertise in the fabrication of micro and nanoparticle with varying size, shapes, stiffnesses, and surface properties.[46] Recently, we have demonstrated that discoidal polymeric nanoconstructs, with mechanical deformability, are able to marginate to blood vessel walls and provide effective therapy for blood clot lysis and tumour chemotherapy, while avoiding clearance by macrophages.[47–49] Here we investigate Pickering emulsions stabilised by anisotropic PLGA DPNs of different sizes. The particles are characterized by scanning electron microscopy (SEM), multisizer, and ζ-potential, then subsequently used to stabilise emulsions of pharmaceutically important medium chain triglyceride (MCT) oil. Resulting drop size, emulsion stability, and 3 phase contact angle are investigated with respect to DPN size. To the best of our knowledge, this is the first example of a Pickering emulsion with non-spherical PLGA particles. By assessing the feasibility of using size tunable discoidal and biodegradable particles as stabilisers, we hope these studies pave the way for future pharmaceutical and consumer applications of PLGA-based Pickering emulsions.

EXPERIMENTAL

Materials

Poly(D,L-lactide-*co*-glycolide) acid (PLGA, lactide:glycolide 50:50, Mw 38,000−54,000 g mol^{-1}), Poly(vinyl alcohol) (PVA, 98% hydrolysed, Mw 31,000−50,000 g mol^{-1}), curcumin ((E,E)-1,7-bis(4-Hydroxy-3-methoxyphenyl)-1,6-heptadiene-3,5-dione), and chloroform were purchased

from Sigma-Aldrich. Polydimethylsiloxane (PDMS) (Sylgard 184) was purchased from Dow Corning Corp. Rhodamin-B lipid (RhB-lipid) was purchased from Avanti Polar Lipids. The oil phase used in Pickering emulsion formulations was medium chain triglyceride (MCT) oil (C6:0 2%, C8:0 50-65%, C10:0 30-45%, C12:0 3%) (VWR), with density at 20 °C of 0.95 g/cm^3.

Discoidal polymeric nanoconstruct fabrication

DPN fabrication proceeded following adaptation of our previously reported process.[48] A master template is fabricated from a silicon wafer with direct laser writing of a photoresist with subsequent deep silicon etching via a Bosch process reactive-ion etching, giving a template with an array of circular wells of 1, 2, and 5 μm diameters with a depth of 0.4, 0.6, and 1 μm respectively. A PDMS inverse template is formed from the master by covering with PDMS and elastomer (10:1, volume ratio), the air bubbles were removed under vacuum, and the PDMS is cured at 80 °C for 3 hours. After removing the PDMS from the silicon, a PVA solution (10 wt% in deionised water) is added on top of the pattern, and placed in an oven at 60 °C for 3 hours. The resulting PVA film is a replica of the silicon master template, after removal from the PDMS. A solution of PLGA in chloroform (150 mg mL^{-1}) is spread over the PVA template wells, and left to stand to allow solvent evaporation. The PVA is dissolved in water and the resulting particles collected after with a filtration step and centrifugation, resuspending in deionised water and centrifuging again. Lipid rhodamine B (2 μL of 1 mg/mL chloroform solution) is added to the polymeric solution composing the DPNs, in order to achieve fluorescent particles. Average size and size distribution were obtained with a Multisizer 4 Coulter counter (Beckman Coulter) with a 20 μm capillary, following the manufacturer's guidelines. Particle sizes were measure in triplicate: the average of the mean size from each measurement for the 1, 2, and 5 μm DPNs was 0.778 ± 0.045 μm, 0.973 ± 0.053 μm, and 1.93 ± 0.129 μm, respectively. Scanning electron microscopy was performed from an air dried drop of DPNs on silica, after uniform gold sputter coating of 10 nm thickness, with a JEOL JSM-6490LA SEM Analytical (low-vacuum) scanning electron microscope (5-15 keV). Size from SEM was calculated as mean ±SD, from sample n=20. A Malvern Nano ZS was used to characterize the zeta (ζ) potential of nanoparticles in deionized water at pH 7.0, in triplicate. DPNs in the PVA particle templates, but before dissolution, were imaged with a Nikon A1 confocal microscope with 63X oil immersion objective.

Formation of DPN pickering emulsions

Primary oil-in-water dispersions were formed at an oil:aqueous phase volume ratio of 20:80 with an ultrasound bath (Branson 2800 ultrasonic bath at 40kHz), at a total volume of 450 μL in glass vials. Aqueous DPN solutions were prepared at 5 mg in 50 uL and this solution was added to the primary emulsion and vortex mixed at high speed for 1 minute, or until no further change in the opacity could be seen. This formulation gave a final emulsion with and oil:aqueous phase volume ratio of 18:82, and a DPN concentration of 10 mg/mL. Curcumin was used in the oil phase as a model active ingredient, that would also allow fluorescent imaging of the oil phase. Rhodamine B lipid used in DPNs allowed imaging of the particle emulsifiers. Emulsions were prepared and characterized at room temperature. Imaging of emulsions was performed with an epi-fluorescent inverted microscope from Leica (model DMI6000). A droplet of sample emulsion (prediluted 1 in 5 times in water) was placed on a glass slide. Curcumin green fluorescence was observed with 488 nm excitation and 525/50 filter set. Rhodamine red fluorescence was observed with 561 nm laser excitation, and 630/75 filter set. Mean droplet diameters, and standard deviation of mean, were determined by image analysis of emulsion microscopy images with approximately 200 droplets measured for each sample. Coefficient of variation was calculated as $CV(\%) = (\sigma/\mu) \times 100$, where: σ is the standard deviation and μ is the mean droplet diameter.

Contact angle

The influence of different particle sizes on the oil water contact angle was measured. A film of particles was formed on a surface of silica by depositing a 30 μL drop of DPNs in water at approximately 20 mg mL^{-1} concentration and leaving to dry for 24 hr protected from dust. The layer of PLGA DPNs was checked to be not soluble in MCT oil. A 5 μL droplet of water was deposited on the DPN film in a continuous phase of MCT oil (densities of 0.95 g cm^{-3} MCT oil and 1 g cm^{-3} deionised water), and an image of the drop shape acquired. The image was processed in ImageJ using the available Contact-Angle jar plugin, to obtain the three phase contact angle values. Measurements were repeated on three separate occasions, and average values with standard deviations calculated.

Pickering emulsion stability assay

The samples were photographed over time to observe any emulsion destabilisation phenomena - creaming, flocculation, coalescence, or any remaining DPN sedimentation. Droplet size was also measured at various timepoints after emulsion formation. Stability imaging of emulsions was performed with an epi-fluorescent inverted microscope from Leica model Leica DMI6000, in brightfield. A droplet of sample emulsion (prediluted 1 in 5 times in water) was placed on a glass slide. Average droplet diameters were determined by image analysis of emulsion microscopy images, with approximately 200 droplets measured for each sample.

RESULTS AND DISCUSSION

Particle fabrication and characterisation

Poly(D,L-lactide-*co*-glycolide) (PLGA) of molecular weight 38,000−54,000 g mol^{-1} and equal molar ratio of co-monomers was used to form disk shaped particles of varying sizes (the process is visually summarized in **Figure 1a**). Firstly, a silica master template was formed for each particle size, with direct laser writing lithography. Nominal dimensions of the particle wells (diameter × depth) were 1 μm × 0.4 μm, 2 μm × 0.6 μm, 5 μm × 1 μm. Poly(dimethylsiloxane) (PDMS) inverse molds were then created from the master templates. A solution of 10% w/v poly(vinylalcohol) (98% hydrolysed, molecular weight 31,000 - 50,000 g mol^{-1}) in water could be applied to the PMDS template and placed at 60 °C for 3 hours, then removed from the mold. The process gives water soluble sacrificial templates which replicate the same dimensions as the master templates. PLGA solution in chloroform was spread over the PVA template wells, and after solvent evaporation and PVA dissolution, particles could be collected and purified. Lipid Rhodamine B (RhB) was added to the PLGA solution, in order to achieve fluorescent particles through direct loading. Microscopy images of the filled PVA particle templates are shown in **Figure S1**.

DPN size in solution was measured with Multisizer 4e in triplicate, which measures fluid impede conductance as particles flow through an aperture (**Figure 1b**). DPNs gave size distributions with

means of 0.778 ±0.045, 0.973 ±0.053, and 1.93 ±0.129 μm for the nominally 1, 2, and 5 μm DPNs, respectively. The average sizes are smaller than the diameter of the particles, because of their anisotropic shape and non-uniform orientation as they flow through the measurement aperture. SEM microscopy was also used to analyse particle size and morphology (**Figure 1c**). With this measurement, particles resembled the size and shape of the PVA template much more closely, particle diameters of 1.18 ±0.091, 2.22 ±0.104, and 5.45 ±0.220 μm were obtained. It is noteworthy that DPNs are highly uniform, such control over particle morphology and uniformity is an advantage of the top-down fabrication strategy. ζ-potential of the fabricated DPNs is shown in **Figure S2**. The average ζ-potentials become slightly more negative with increasing particle diameters (i.e. surface), from -17.5 mV for 1 μm DPNs to -21.2 mV for the 5 μm DPN sample, due to the presence of carboxylic acid end groups on the polymer chains.

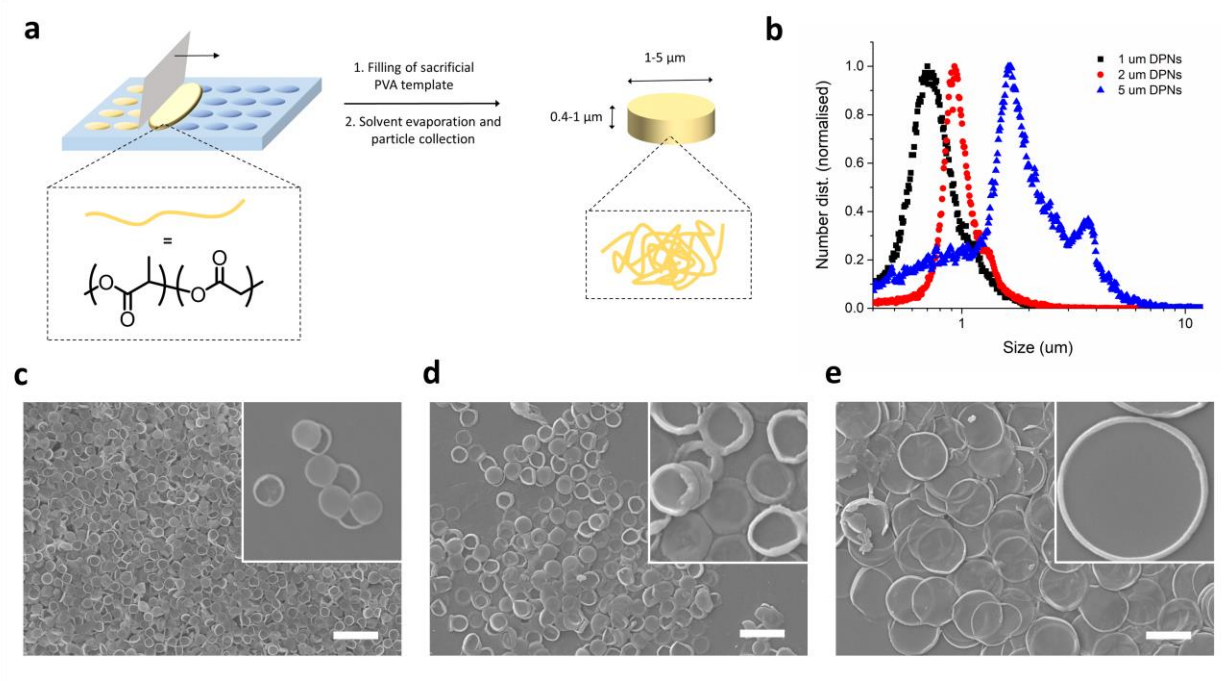

***Figure 1. Fabrication and characterization of PLGA DPN**. **a)** Outline of the particle synthesis scheme for the formation of DPNs through a lithographic templating process, **b)** Representative size distributions of the particles in solution via Multisizer, **c)** SEM image of 1 μm DPNs, **d)** SEM image of 2 μm DPNs, **e)** SEM image of 5 μm DPNs. (Scale bars 5 μm, inset size 6 × 6 μm).*

Pickering emulsion formation

The high degree of control over size allows the authors to investigate the role of DPNs as Pickering emulsifiers. Platelet and disk shaped particles are particularly interesting for this application as their high surface areas can readily lower the interfacial tension of droplets.[50] Previous research has investigated disk shaped clay and cellulose particles,[51] and more recently block copolymer platelet particles, as oil-in-water and water-in-water emulsifiers.[52] However, compared to our top-down approach, these bottom-up designed particle systems present difficulties in precisely controlling the shape, size and polydispersity.[53]

We then investigated the ability of PLGA DPNs to stabilise oil-in-water emulsions. Medium chain triglyceride oil (Miglyol) was chosen as the oil phase, due to its use in a variety of FDA approved pharmaceutical/food/cosmetic products. It is immiscible with water and has an interfacial tension of 26.5 mN m^{-1}.[54] Primary oil-in-water dispersions were formed at an oil: aqueous phase volume ratio of 20:80, and concentrated aqueous DPN solutions added to the primary emulsion and vortex mixed. The hydrophilic DPNs attach to the interface from the water phase and stabilise the emulsion. The vortex mixing was continued for 1 minute to allow equilibrium state to be reached. A final emulsion with and oil:aqueous phase volume ratio of 18:82, and final DPN concentration of 10 mg mL^{-1} was achieved.

The mean droplet size distribution formed with different DPN configuations was used to characterise the emulsion formation, as seen in **Figure 2**. Analysis of the obtained optical microscopy images allows for the systematic measurement of both stable and unstable emulsions, compared to some other diffraction or scattering based droplet size measurements. Smaller mean droplet sizes of Pickering emulsions were documented for smaller DPNs, at the same particle concentration by mass. Emulsions from 1 μm DPNs gave a mean droplet size of 51 ±24 μm, 2 μm DPNs gave 121 ±51 μm, and 5 μm DPNs returned a mean droplet size of 730 ±223 μm. The droplet polydispersity is large for all DPN configurations, likely due to the vortex mixing during emulsification (coefficient of variation = 48%, 42%, and 31%, for the 1, 2, and 5 μm DPNs respectively). Similar trends have been reported previously, Binks and Lumsdon observed a positive correlation between particle stabiliser size and droplet size, with spherical polystyrene

beads of 1.1, 3.2, and 6.1 μm diameters giving mean droplet diameters of around 40, 60, and 75 μm respectively.[34] An increase in droplet size and polydispersity has also been observed with non-spherical particles compared to spherical particles of the same composition.[42,55]

Upon inclusion of the red fluorescent lipid-RhB molecules in the PLGA matrix of the DPN, we could observe the localization of the particles at the droplet surface. This is particularly notable for the 1 μm and 2 μm particles, which appear to interact strongly with the oil-water interface, with surface coverages estimated to be above approximately 50%. **Figure 2f** shows a fluorescence length profile across approximately 100 μm covering one MCT oil droplet stabilised by 1 μm DPNs. The red fluorescence is contained to the droplet edges, indicating that the DPNs are indeed located at the oil-water interface. Emulsions stabilised by the largest 5 μm DPNs, were unstable, and droplet polydispersity was indeed high. DPN surface coverage appeared to be less than for the smaller DPNs, with less red fluorescence around the outside of droplets. In all cases there was a fraction of particles in the water phase, which we hypothesise is due to the hydrophilic nature of the particles with negative surface ζ-potential.

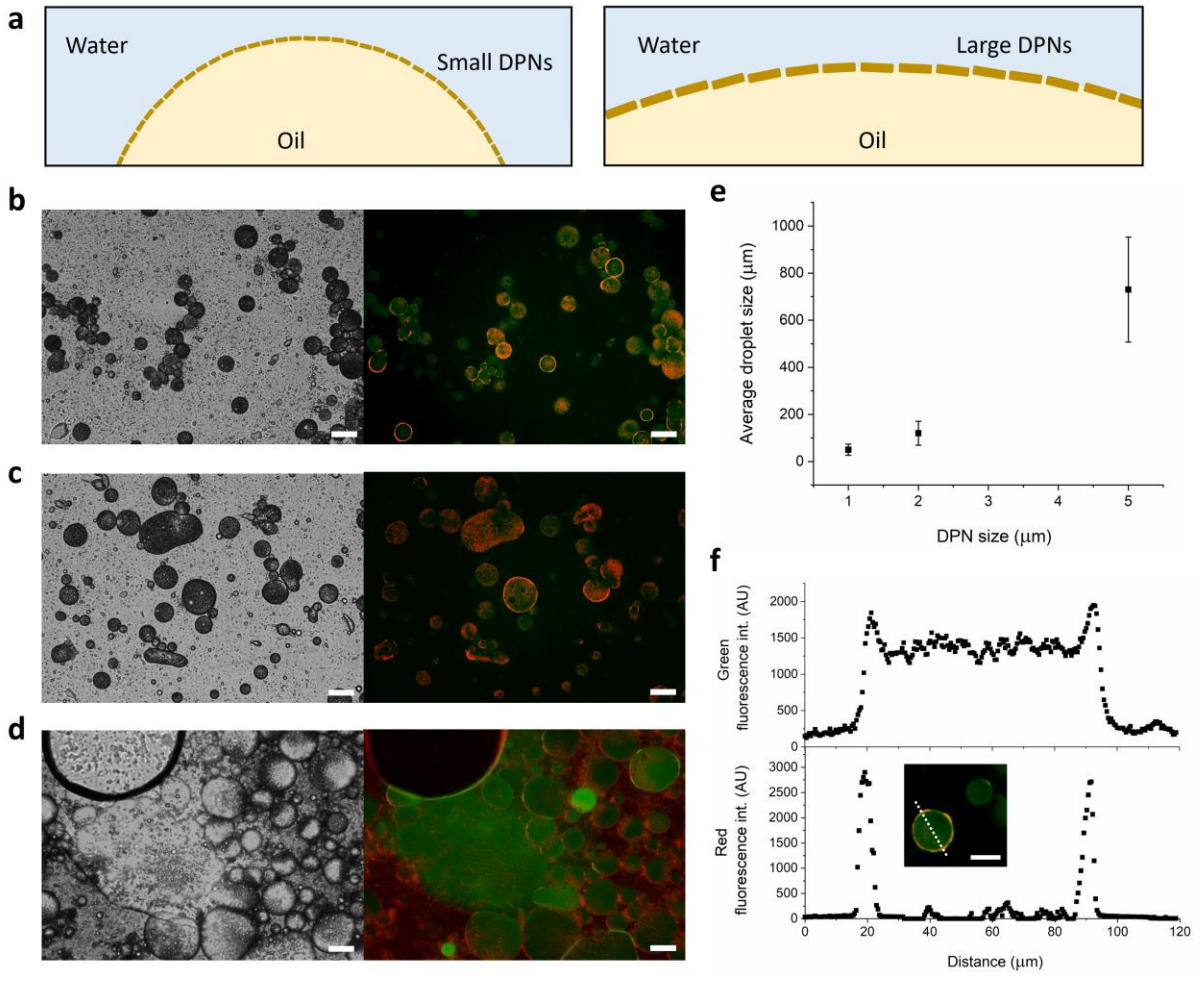

Figure 2. Formation and characterisation of DPN stabilised oi-in-water emulsions*. **a)** Schematic of DPN interaction with oil-water interface, in case of small and large DPNs. The red color derives from the dispersion of RhB-lipid chanins within the PLGA matrix of DPNs, **b)** Fluorescent microscopy images of DPN stabilised oil-in-water emulsions (red = RhB-DPN, green: curcumin loaded in MCT oil phase) with 1 µm DPNs, **c)** with 2 µm DPNs, **d)** with 5 µm DPNs (Scale bars: 100 µm), **e)** Emulsion droplet size in relation to DPN particle size, **f)** Fluorescence profiles of red and green channels across an individual droplet (stabilised by 1 µm DPNs) (Scale bar: 50 µm).*

Particle-interface interaction

The wettability or hydrophilicity of PLGA DPNs was evaluated with three phase contact angle (shown in **Figure 3** and **S3**). A drop of water (5 μL) was deposited on a surface layer of DPN particles in a continuous phase of MCT oil. DPNs are assumed to be oriented lying flat to the silica surface during the measurement (as seen in **Figure 1**), although there could be multiple layers of particles and the packing arrangement will not be the same as when the particles are at a fluid-fluid interface. Particles were checked to be insoluble in MCT oil, regardless of the polymer chains not being covalently crosslinked. For the 1 μm DPNs, a contact angle of approximately 85°±7° was documented. This indicates interaction with both aqueous and oil phases, with a slight preference for water, and a good ability to stabilise emulsions (theoretical maximum stability with a contact angle of 90°). The contact angle decreased with increasing DPN diameter being about 77°±13° for the 2 μm DPNs, and about 68°±12° for the 5 μm DPNs. This decrease in contact angle has to be ascribed to the particles being more hydrophilic with larger surface areas exposed to water.

It is important to note that the layer of surface deposited DPNs, in these contact angle measurements, may not be a monolayer aligned parallel to the interface. The surface particles could also be at varying orientations, which could affect the contact angle readings to an unknown extent. For example, disks orientated perpendicular to the interface would give contact angles measurements closer to 90°, while a very thin disk oriented with its base in contact with the interface would give a contact angle closer to zero.

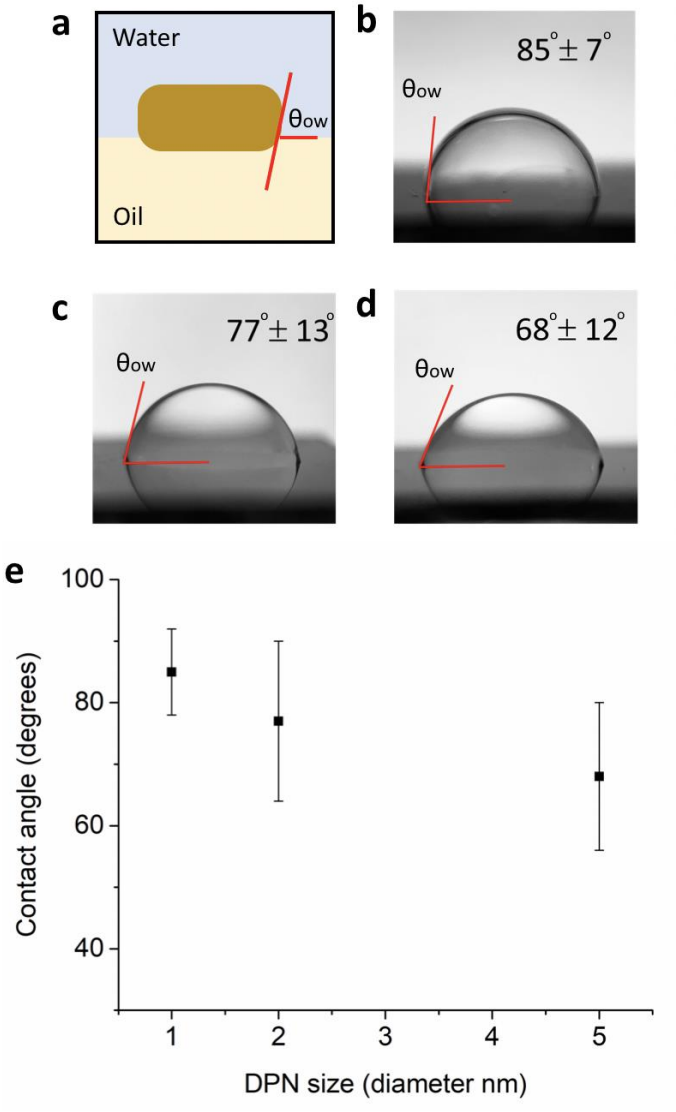

Figure 3. Three phase contact angle measurements, a) *Schematic showing the assumption for the DPN orientation at the oil-water interface – DPN major axis is tangent to the interface,* ***b)*** *Representative images of contact angle of 5 μL droplet of water in MCT oil continuous phase, on a film of DPN particles of size 1 μm,* ***c)*** *DPNs of size 2 μm,* ***d)*** *DPNs of size 5 μm,* ***e)*** *Plot of contact angle against DPN size, results are plotted as mean ±SD (n=3).*

Emulsion stability study

To assess the effect of DPN size on emulsion stability, fresh emulsions were prepared at water: oil volume fractions 82:18, with 10 mg mL^{-1} DPN concentration. Images of the emulsions over time (seen in **Figure 4a**), show that the 1 μm and 2 μm DPN stabilised emulsions were homogenous up to approximately 24 hours. After 24 hours separation of the oil and water phases can be seen, and an increase in red colour at the bottom of the vials indicating particle sedimentation. Images of the 5 μm particle stabilised emulsion show phase separation after 24 hours. DPN sedimentation due to gravitational forces would be higher for the 5 μm particles, and is the likely a contributing factor to this destabilisation, and can be seen at 96 hours. We hypothesise that this particle sedimentation and desorption from the oil-water interface then leads to increased droplet aggregation and coalescence. Although coalescence appears to be the major route of destabilisation, Ostwald ripening is another destabilisation process which could be occurring. Smaller droplets would gradually become larger due to diffusion of MCT oil molecules of the dispersed phase through the aqueous phase.[56]

In addition, droplet size over time was investigated with optical microscopy at 6 hours, 12 hours, and 24 hours for the three DPN sizes **(Figure 4b** and **4c**). For the 1 μm emulsion, MCT oil droplets remained spherical in shape and increased in mean diameter slightly from 74 μm, at formation, to 140 μm, after 24 hours. The 2 μm DPN stabilised emulsion had an increase in droplet size from 97 μm to 345 μm, after 24 hours. In the case of 5 μm DPN stabilised emulsions, the mean droplet size already started at 603 μm and became too large to accurately measure with microscopy after already 6 hours. Oil droplets of the 2 μm DPN stabilised sample exhibited a slight loss of spherical shape, while 5 μm stabilised emulsion droplets showed some non-spherical droplets even directly after emulsification.

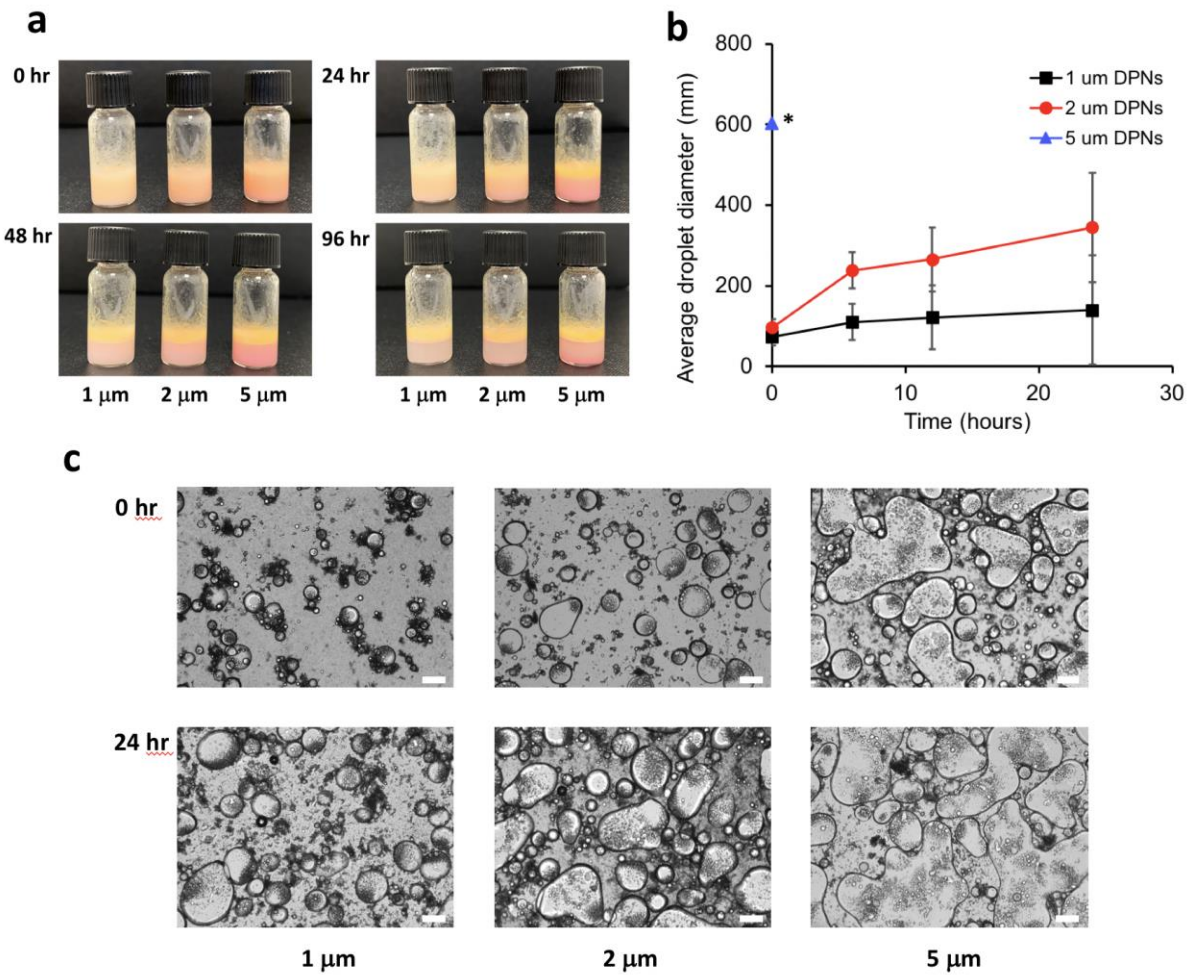

Figure 4. DPN stabilised emulsion stability study. a) *Photographs of emulsion appearance after 0, 24, 48, and 96 hr,* ***b)*** *Plot of droplet size over 24 hr after emulsion formation (* refers to samples after time zero showed coalescence affecting droplet size measurements),* ***c)*** *Optical microscopy images of emulsions at 0 and 24 hr (Scale bars 100 µm).*

Pickering emulsion formation and stability depends on and can be greatly affected by the interaction strength of the particle at the oil-water interface. The attachment of particles to the fluid-fluid interface is usually favourable due to a reduction in the area of the planar fluid-fluid interface normally of high interfacial tension.[57] For particles spontaneously accumulating at these interfaces, detachment (or attachment) free energy can be calculated as a function of the surface areas exposed to the respective fluid phases, volume of each fluid phases, and the surface tension. In this case, we assume the interface is flat as compared to the particle size. The free energy of

detachment is the difference between the energy of the system before and after desorption (or absorption for the attachment energy).[50,58] If ΔG_{dw} is the free energy of particle detachment into water, G_I is the free energy of the particle at the interface, and G_w is the free energy of the particle in the water phase, then it follows that

$$\Delta G_{dw} = G_I - G_w \qquad \text{(eq. 1)}$$

When a spherical particle is aligned at a planar oil-water interface in equilibrium, the surface free energy of the system is at a minimum and is given by (***eq. 2)***:

$$\Delta G_{dw} = \pi r^2 \gamma_{ow} (1 - cos\theta_{ow})^2 \qquad \text{(eq. 2)}$$

where γ_{ow} is the oil-water interfacial tension and θ_{ow} is the particle-oil-water contact angle. When a disk shaped particle is considered, the area involved in the force balance differs from the case of a sphere, and two geometric parameters are needed to account for the particle geometry.[50] The attachment energy does also depend on the particle orientation. For the following calculations, we assume that DPNs are orientated flat to the oil-water interface in a monolayer, and that the particles have hemispherical edges. The free energy of detachment into the water phase then follows ***(eq. 3)***:

$$\Delta G_{dw} = \pi b^2 (1 - cos\,\theta_{ow})^2 \gamma_{ow} \left[1 + \frac{\left(\frac{a}{b} - 1\right)^2}{1 - cos\theta_{ow}} + \frac{2(\frac{a}{b} - 1)(sin\theta_{ow} - \theta_{ow} cos\theta_{ow})}{(1 - cos\theta_{ow})^2}\right] \qquad \text{(eq. 3)}$$

where the MCT oil-water interfacial tension γ_{ow} is taken as 26.5 mN m^{-1},[54] the contact angle θ_{ow} is the measured values as from **Figure 3**, and the geometric parameters *a* and *b* are shown and listed in **Figure S5** for the different DPN configurations.

The attachment energy of solid particles at oil-water interfaces is typically orders of magnitude higher than the thermal energy k_BT, and for larger particles this increases.[57,59,60] ΔG_{dw} was calculated to be 0.132×10^8 k_BT, for 1 μm DPNs; 1.30×10^8 k_BT, for 2 μm DPNs; and 9.42×10^8 k_BT, for 5 μm DPNs. This indicates energetically favourable attachment of micrometer size DPN particles to the MCT oil-water interface. Aveyard *et al.*, showed that the attachment energy of around 10^7 factors of k_BT for spherical polystyrene microparticles of diameter 2.6 μm at ocatane-water interfaces.[59] When compared to these results, our values of around 10^8 k_BT, are slightly

larger, for similar size particles, due to the disk-like shape. This is much larger than the attachment energy for smaller particles, for example, 10 nm silica particles at oil-water interface (50 mN m^{-1}, with a 90° contact angle) give ΔG values of approximately 10^4 k_BT.[60]

From the calculated free energies for particle dettachment, we can see that DPN interaction with oil-water interfaces should be strongly favoured, however we see droplet coalescence and emulsion destabilisation at less than 24 hours. We therefore wanted to determine whether the concentration of particles was enough to sufficiently cover the total surface area. Theoretical maximum surface coverage for disks on a flat surface in a hexagonal packing arrangement is 90.7% while for a square lateral packing it is 78.5% (packing arrangements depicted in **Figure S4**). A number of studies have estimated particle surface coverage in Pickering emulsion to be lower, particularly for large particles (>1 μm). Haney *et al.*, showed that with 440 μm Janus particles, efficient emulsification occurred, however surface on top of the droplets was often free of particles.[61] The authors estimated that emulsion droplets were on average approximately 50% covered by particles.[61] Size of Pickering emulsion droplets was able to be predicted based on the size of the synthesised Janus particles. Researchers have also calculated surface coverage for colloidal silica particles in Pickering emulsions. A monolayer of particles with 54% surface coverage was found to be coating the oil droplets.[62] In this case the limitation was due to random jamming phenomena. In cases of incomplete surface coverage, the overall mass balance can be described by ***(eq. 4)***, where C_0 is total concentration of particles in the system in g g^{-1} (with respect to the amount of water), C_{surf} is the concentration of particles at the oil-water interface (with respect to the amount of water), and C_{excess} is the concentration of excess particles in the continuous water phase.

$$C_0 = C_{surf} + C_{excess} \qquad \text{(eq. 4)}$$

The equation can be further expanded by considering the total surface area of the oil-water interface, and the surface area covered by disk particles. This was demonstrated for clay Laponite disk particles in Pickering miniemulsion polymerization by Bon *et al*., in which case the equation could be expressed as shown in ***(eq. 5)***,

$$C_{excess} = C_0 - \sqrt{3}\pi \left(\frac{\rho_{part}}{\rho_{oil}}\right)\left(\frac{h}{d_{oil}}\right) C_{oil} \qquad \text{(eq. 5)}$$

when assuming full surface coverage, droplet and particle monodispersity, and no surface curvature.[63] ρ_{part} and ρ_{oil} are the densities of the particle and oil respectively, h is the height of the discoidal particle while d is the diameter of the oil droplet, and C_{oil} is the total concentration of oil in the system. The $\sqrt{3\pi}$ (= 5.441) factor relates to the hexagonal packing. It would be $3\pi/2$ (= 4.712) for a square lateral packing. Then, *w*e can calculate C_{excess} - the excess concentration of particles in the water phase - by using our experimental values for C_0, C_{oil}, h of each particle configurations , d_{oil} from microscopy, and a value of PLGA density ρ_{part} of 1.34 g cm^{-3},[64] and MCT oil density ρ_{oil} of 0.95 g cm^{-3}. For emulsions stabilised with a fixed C_0 concentration of particles, the amount of excess particles in the water phase increases with increasing DPN particle size. If we assume a surface coverage of 50%, C_{excess} increases from 0.00512 g g^{-1} for 1 μm DPNs to 0.0110 g g^{-1} for 5 μm DPNs, with the total particle concentration being 0.0122 g g^{-1}. This demonstrates that with larger DPNs, and as d_{oil} increases, a higher proportion of DPNs are in excess of the amount needed to cover 50% of the droplet surface and remain in the aqueous phase. The trend remains if we assume square lateral or hexagonal packing densities. Interestingly, at the highest possible monolayer packing density, hexagonal, with 1 μm DPNS and emulsion droplets of 51 μm, there is a small insufficiency of DPNs to cover the interface.

Table 1. DPN stabilised emulsion values for free energy of particle detachment and particle concentrations relative to water (total and excess).

Emulsion sample	ΔG_{dw} (x10^8 k_BT)	C_0 (g g^{-1})	C_{excess} (g g^{-1}) [a]	C_{excess} (g g^{-1}) [b]	C_{excess} (g g^{-1}) [c]
1 μm DPN	0.132	0.0122	0.00512	0.00109	-0.000632
2 μm DPN	1.30	0.0122	0.00778	0.00525	0.00418
5 μm DPN	9.42	0.0122	0.01100	0.01030	0.01000

[a] = assuming 50% surface coverage, [b] = assuming 78.5% surface coverage (square lateral packing), [c] = assuming 90.7% surface coverage (hexagonal packing).

It is important to note that particle orientation might not be flat on the interface. This would affect both the contact angle and the concentration of excess particles. The packing of disks with their largest surface area face perpendicular to the oil water interface (rather than parallel as considered for the majority of the analysis), would increase the packing density significantly. A higher

concentration of particles would be needed to cover the interface surface, reducing C_{excess}.[6,65] Finally, Pickering emulsion polymerization of methyl methacrylate (MMA) was also attempted using the 1 μm PLGA DPNs, however the polymerisation proceeded in the dispersed state with no emulsification, which was found to be due to the particles dissolving in the MMA monomer phase. Further work could investigate DPN stabilised emulsion polymerizations of other monomers.

Interestingly, the relationships in ***eq. 2*** and ***eq. 3*** above, do not take in to consideration gravity. While this is standard for emulsions stabilised by nanometer sized particles, work by Cates, Clegg and others, have shown the importance of gravitational fields on the stability of micrometer sized particle-stabilised emulsions.[61,66,67] Over time microparticles have been observed to fall to the sides and bottoms of emulsion droplets, with a fraction of the interfacially adsorbed particles detaching. We hypothesise gravity is affecting emulsion stability, at large DPN size, despite the strong particle attachment energies calculated in this manuscript.

CONCLUSIONS

We investigated the use of solid PLGA discoidal particles as emulsion stabilisers and the impact of particle size on emulsion characteristics. DPNs of diameter 1, 2, and 5 μm were fabricated with a template based lithography process, previously establish by our group for producing particles of differing size and shapes. Emulsions were formed at 1 wt% particles with MCT oil, commonly used for pharmaceutical formulations, as the dispersed phase. Observation of mean droplet diameter was used to infer information about emulsification efficiency, with droplet size and dispersity increasing with particle size. In addition, RhB-lipid encapsulated in the DPNs allowed fluorescent microscopy visualization and showed that DPNs were present at the oil-water interface. Emulsion stability was assessed by monitoring both visual emulsion appearance and mean droplet size with microscopy. DPN stabilised emulsion were stable around 24 hours or less in the case of 1 μm and 2 μm DPNs and 6-12 hours in case of 5 μm DPNs.

Wettability of the particles in this emulsion system was assessed by measuring the contact angle, with particle 'hydrophilicity' increasing with particle size, as shown by contact angles decreasing from 85° to 68°, from 1 μm to 5 μm DPNs. Finally, based on Pickering emulsion theory, calculations of ΔG_{dw}, the free energy of particle detachment, and C_{excess}, the proportion of excess

particles not interacting with the interface, were calculated. The results indicate that while the energy of attachment for disk shaped particles of this size is significant, emulsion stability is affected by gravitational forces and coalescence. From these studied examples, we conclude that there is balancing of favourable and unfavourable forces for Pickering emulsions stabilised with larger DPNs, with particles sizes of 1 μm being promising.

Future research should look more closely at DPN packing and arrangement at the oil-water interface. High resolution cryo-SEM microscopy would be beneficial to further determine surface coverage of DPNs on oil droplets. Due to larger DPNs being less stable over time because of particle sedimentation, it would be interesting to investigate smaller DPN size as Pickering emulsifiers. There is likely an inflection point in ideal DPN size between 100 nm and 1 μm, were larger DPNs have stronger interface interaction energy yet, small enough to avoid gravitational instability. Fabrication of DPNs smaller than 1 μm diameter is challenging with the current direct laser writing lithography master template formation. Applications of PLGA DPN stabilised MCT oil emulsions can be envisioned in drug delivery and pharmaceutics. PLGA DPNs could have the following benefits in these applications: 1) Controlling release of drug from oil droplets by tuning surface coverage of droplets, and thus the ability of molecules to diffuse from MCT oil into the aqueous phase (a similar concept described by Prestidge *et al*.)[68], 2) Use for combination therapies, with different rates of drug release by encapsulating one active ingredient in the oil phase, and one in the PLGA polymer DPNs.

ACKNOWLEDGEMENTS

This work was partially supported by the European Research Council under the European Union's Seventh Framework Programme (FP7/2007-2013)/ERC grant agreement no. 616695 and by the European Union's Horizon 2020 research and innovation program under the Marie Sklodowska-Curie grant agreement no. 754490.

CRediT author contributions

A.B.C.: Conceptualization, Methodology, Investigation, Writing - Original Draft, Writing - Review & Editing. M.S.: Investigation, Writing - Original Draft, Writing - Review & Editing.

P.N.M.: Conceptualization, Writing - Review & Editing. T.L.M.: Methodology Writing - Review & Editing. A.L.P.: Methodology, Writing - Review & Editing. P.D.: Supervision, Funding acquisition, Writing- Reviewing and Editing.

REFERENCES

(1) Albert, C.; Beladjine, M.; Tsapis, N.; Fattal, E.; Agnely, F.; Huang, N. Pickering Emulsions: Preparation Processes, Key Parameters Governing Their Properties and Potential for Pharmaceutical Applications. *J. Controlled Release* **2019**, *309*, 302–332.

(2) Pham, A. C.; Peng, K.-Y.; Salim, M.; Ramirez, G.; Hawley, A.; Clulow, A. J.; Boyd, B. J. Correlating Digestion-Driven Self-Assembly in Milk and Infant Formulas with Changes in Lipid Composition. *ACS Appl. Bio Mater.* **2020**, *3* (5), 3087–3098. https://doi.org/10.1021/acsabm.0c00131.

(3) Gurnani, P.; Sanchez-Cano, C.; Abraham, K.; Xandri-Monje, H.; Cook, A. B.; Hartlieb, M.; Lévi, F.; Dallmann, R.; Perrier, S. RAFT Emulsion Polymerization as a Platform to Generate Well-Defined Biocompatible Latex Nanoparticles. *Macromol. Biosci.* **2018**, *18* (10), 1800213. https://doi.org/10.1002/mabi.201800213.

(4) Gurnani, P.; Cook, A. B.; Richardson, R. A. E.; Perrier, S. A Study on the Preparation of Alkyne Functional Nanoparticles via RAFT Emulsion Polymerisation. *Polym. Chem.* **2019**, *10* (12), 1452–1459. https://doi.org/10.1039/C8PY01579A.

(5) Wu, J.; Ma, G.-H. Recent Studies of Pickering Emulsions: Particles Make the Difference. *Small* **2016**, *12* (34), 4633–4648.

(6) Ballard, N.; Law, A. D.; Bon, S. A. F. Colloidal Particles at Fluid Interfaces: Behaviour of Isolated Particles. *Soft Matter* **2019**, *15* (6), 1186–1199.

(7) Ramsden, W.; Gotch, F. Separation of Solids in the Surface-Layers of Solutions and 'Suspensions' (Observations on Surface-Membranes, Bubbles, Emulsions, and Mechanical Coagulation).—Preliminary Account. *Proc. R. Soc. Lond.* **1904**, *72* (477–486), 156–164.

(8) Pickering, S. U. CXCVI.—Emulsions. *J. Chem. Soc. Trans.* **1907**, *91* (0), 2001–2021.

(9) Zoppe, J. O.; Venditti, R. A.; Rojas, O. J. Pickering Emulsions Stabilized by Cellulose Nanocrystals Grafted with Thermo-Responsive Polymer Brushes. *J. Colloid Interface Sci.* **2012**, *369* (1), 202–209.

(10) Chen, Z.; Zhou, L.; Bing, W.; Zhang, Z.; Li, Z.; Ren, J.; Qu, X. Light Controlled Reversible Inversion of Nanophosphor-Stabilized Pickering Emulsions for Biphasic Enantioselective Biocatalysis. *J. Am. Chem. Soc.* **2014**, *136* (20), 7498–7504.

(11) Gerth, M.; Voets, I. K. Molecular Control over Colloidal Assembly. *Chem. Commun.* **2017**, *53* (32), 4414–4428.

(12) Flores, J. A.; Jahnke, A. A.; Pavia-Sanders, A.; Cheng, Z.; Wooley, K. L. Magnetically-Active Pickering Emulsions Stabilized by Hybrid Inorganic/Organic Networks. *Soft Matter* **2016**, *12* (46), 9342–9354.

(13) Dinsmore, A. D.; Hsu, M. F.; Nikolaides, M. G.; Marquez, M.; Bausch, A. R.; Weitz, D. A. Colloidosomes: Selectively Permeable Capsules Composed of Colloidal Particles. *Science* **2002**, *298* (5595), 1006–1009. https://doi.org/10.1126/science.1074868.

(14) Wang, Z.; van Oers, M. C. M.; Rutjes, F. P. J. T.; van Hest, J. C. M. Polymersome Colloidosomes for Enzyme Catalysis in a Biphasic System. *Angew. Chem. Int. Ed.* **2012**, *51* (43), 10746–10750. https://doi.org/10.1002/anie.201206555.

(15) Geest, B. G. D.; Koker, S. D.; Demeester, J.; Smedt, S. C. D.; Hennink, W. E. Self-Exploding Capsules. *Polym. Chem.* **2010**, *1* (2), 137–148. https://doi.org/10.1039/B9PY00287A.

(16) Wijk, J. van; Heunis, T.; Harmzen, E.; Dicks, L. M. T.; Meuldijk, J.; Klumperman, B. Compartmentalization of Bacteria in Microcapsules. *Chem. Commun.* **2014**, *50* (97), 15427–15430. https://doi.org/10.1039/C4CC04901B.

(17) Jutz, G.; Böker, A. Bio-Inorganic Microcapsules from Templating Protein- and Bionanoparticle-Stabilized Pickering Emulsions. *J. Mater. Chem.* **2010**, *20* (21), 4299–4304. https://doi.org/10.1039/B925018B.

(18) Liu, F.; Tang, C.-H. Soy Glycinin as Food-Grade Pickering Stabilizers: Part. III. Fabrication of Gel-like Emulsions and Their Potential as Sustained-Release Delivery Systems for β-Carotene. *Food Hydrocoll.* **2016**, *56*, 434–444. https://doi.org/10.1016/j.foodhyd.2016.01.002.

(19) Alison, L.; Demirörs, A. F.; Tervoort, E.; Teleki, A.; Vermant, J.; Studart, A. R. Emulsions Stabilized by Chitosan-Modified Silica Nanoparticles: PH Control of Structure-Property Relations. *Langmuir* **2018**, *34* (21), 6147–6160.

(20) Yang, Y.; Fang, Z.; Chen, X.; Zhang, W.; Xie, Y.; Chen, Y.; Liu, Z.; Yuan, W. An Overview of Pickering Emulsions: Solid-Particle Materials, Classification, Morphology, and Applications. *Front. Pharmacol.* **2017**, *8*. https://doi.org/10.3389/fphar.2017.00287.

(21) Kumar, M. N. V. R.; Muzzarelli, R. A. A.; Muzzarelli, C.; Sashiwa, H.; Domb, A. J. Chitosan Chemistry and Pharmaceutical Perspectives. *Chem. Rev.* **2005**, *104*, 6017–6084. https://doi.org/10.1021/cr030441b.

(22) Prestidge, C. A.; Simovic, S. Nanoparticle Encapsulation of Emulsion Droplets. *Int. J. Pharm.* **2006**, *324* (1), 92–100. https://doi.org/10.1016/j.ijpharm.2006.06.044.

(23) Frelichowska, J.; Bolzinger, M.-A.; Pelletier, J.; Valour, J.-P.; Chevalier, Y. Topical Delivery of Lipophilic Drugs from o/w Pickering Emulsions. *Int. J. Pharm.* **2009**, *371* (1), 56–63. https://doi.org/10.1016/j.ijpharm.2008.12.017.

(24) Zhou, Y.; Sun, S.; Bei, W.; Zahi, M. R.; Yuan, Q.; Liang, H. Preparation and Antimicrobial Activity of Oregano Essential Oil Pickering Emulsion Stabilized by Cellulose Nanocrystals. *Int. J. Biol. Macromol.* **2018**, *112*, 7–13. https://doi.org/10.1016/j.ijbiomac.2018.01.102.

(25) Whitby, C. P.; Lim, L. H.; Eskandar, N. G.; Simovic, S.; Prestidge, C. A. Poly(Lactic-Co-Glycolic Acid) as a Particulate Emulsifier. *J. Colloid Interface Sci.* **2012**, *375* (1), 142–147. https://doi.org/10.1016/j.jcis.2012.02.058.

(26) Qi, F.; Wu, J.; Sun, G.; Nan, F.; Ngai, T.; Ma, G. Systematic Studies of Pickering Emulsions Stabilized by Uniform-Sized PLGA Particles: Preparation and Stabilization Mechanism. *J. Mater. Chem. B* **2014**, *2* (43), 7605–7611. https://doi.org/10.1039/C4TB01165A.

(27) Deschamps, F.; Harris, K. R.; Moine, L.; Li, W.; Tselikas, L.; Isoardo, T.; Lewandowski, R. J.; Paci, A.; Huang, N.; de Baere, T.; Salem, R.; Larson, A. C. Pickering-Emulsion for Liver Trans-Arterial Chemo-Embolization with Oxaliplatin. *Cardiovasc. Intervent. Radiol.* **2018**, *41* (5), 781–788. https://doi.org/10.1007/s00270-018-1899-y.

(28) Albert, C.; Huang, N.; Tsapis, N.; Geiger, S.; Rosilio, V.; Mekhloufi, G.; Chapron, D.; Robin, B.; Beladjine, M.; Valérie, N.; Fattal, E.; Agnely, F. Bare and Sterically Stabilized PLGA Nanoparticles for the Stabilization of Pickering Emulsions. *Langmuir* **2018**, *34* (46), 13935–13945. https://doi.org/10.1021/acs.langmuir.8b02558.

(29) Ruhland, T. M.; Gröschel, A. H.; Ballard, N.; Skelhon, T. S.; Walther, A.; Müller, A. H. E.; Bon, S. A. F. Influence of Janus Particle Shape on Their Interfacial Behavior at Liquid-Liquid Interfaces. *Langmuir ACS J. Surf. Colloids* **2013**, *29* (5), 1388–1394. https://doi.org/10.1021/la3048642.

(30) Thompson, K. L.; Fielding, L. A.; Mykhaylyk, O. O.; Lane, J. A.; Derry, M. J.; Armes, S. P. Vermicious Thermo-Responsive Pickering Emulsifiers. *Chem. Sci.* **2015**, *6* (7), 4207–4214. https://doi.org/10.1039/C5SC00598A.

(31) Richtering, W. Responsive Emulsions Stabilized by Stimuli-Sensitive Microgels: Emulsions with Special Non-Pickering Properties. *Langmuir* **2012**, *28* (50), 17218–17229. https://doi.org/10.1021/la302331s.

(32) Lotierzo, A.; Longbottom, B. W.; Lee, W. H.; Bon, S. A. F. Synthesis of Janus and Patchy Particles Using Nanogels as Stabilizers in Emulsion Polymerization. *ACS Nano* **2018**, *13* (1), 399–407. https://doi.org/10.1021/acsnano.8b06557.

(33) Destribats, M.; Lapeyre, V.; Wolfs, M.; Sellier, E.; Leal-Calderon, F.; Ravaine, V.; Schmitt, V. Soft Microgels as Pickering Emulsion Stabilisers: Role of Particle Deformability. *Soft Matter* **2011**, *7* (17), 7689–7698. https://doi.org/10.1039/C1SM05240C.

(34) Binks, B. P.; Lumsdon, S. O. Pickering Emulsions Stabilized by Monodisperse Latex Particles: Effects of Particle Size. *Langmuir* **2001**, *17* (15), 4540–4547. https://doi.org/10.1021/la0103822.

(35) Destribats, M.; Eyharts, M.; Lapeyre, V.; Sellier, E.; Varga, I.; Ravaine, V.; Schmitt, V. Impact of PNIPAM Microgel Size on Its Ability To Stabilize Pickering Emulsions. *Langmuir* **2014**, *30* (7), 1768–1777. https://doi.org/10.1021/la4044396.

(36) Ashby, N. P.; Binks, B. P. Pickering Emulsions Stabilised by Laponite Clay Particles. *Phys. Chem. Chem. Phys.* **2000**, *2* (24), 5640–5646. https://doi.org/10.1039/B007098J.

(37) Voorn, D. J.; Ming, W.; van Herk, A. M. Polymer−Clay Nanocomposite Latex Particles by Inverse Pickering Emulsion Polymerization Stabilized with Hydrophobic Montmorillonite Platelets. *Macromolecules* **2006**, *39* (6), 2137–2143. https://doi.org/10.1021/ma052539t.

(38) Teixeira, R. F. A.; McKenzie, H. S.; Boyd, A. A.; Bon, S. A. F. Pickering Emulsion Polymerization Using Laponite Clay as Stabilizer To Prepare Armored "Soft" Polymer Latexes. *Macromolecules* **2011**, *44* (18), 7415–7422.

(39) Mejia, A. F.; Diaz, A.; Pullela, S.; Chang, Y.-W.; Simonetty, M.; Carpenter, C.; Batteas, J. D.; Mannan, M. S.; Clearfield, A.; Cheng, Z. Pickering Emulsions Stabilized by Amphiphilic Nano-Sheets. *Soft Matter* **2012**, *8* (40), 10245–10253. https://doi.org/10.1039/C2SM25846C.

(40) Inam, M.; Jones, J.; Pérez-Madrigal, M.; Arno, M. C.; Dove, A. P.; O'Reilly, R. Controlling the Size of Two-Dimensional Polymer Platelets for Water-in-Water Emulsifiers. *ACS Cent. Sci.* **2017**, *4* (1), 63–70. https://doi.org/10.1021/acscentsci.7b00436.

(41) Vis, M.; Opdam, J.; Oor, I.; Soligno, G.; Roij, R.; Tromp, R.; Erné, B. Water-in-Water Emulsions Stabilized by Nanoplates. *ACS Macro Lett.* **2015**, *4*, 965–968. https://doi.org/10.1021/acsmacrolett.5b00480.

(42) Madivala, B.; Vandebril, S.; Fransaer, J.; Vermant, J. Exploiting Particle Shape in Solid Stabilized Emulsions. *Soft Matter* **2009**, *5* (8), 1717–1727. https://doi.org/10.1039/B816680C.

(43) Kalashnikova, I.; Bizot, H.; Bertoncini, P.; Cathala, B.; Capron, I. Cellulosic Nanorods of Various Aspect Ratios for Oil in Water Pickering Emulsions. *Soft Matter* **2012**, *9* (3), 952–959. https://doi.org/10.1039/C2SM26472B.

(44) Peddireddy, K. R.; Nicolai, T.; Benyahia, L.; Capron, I. Stabilization of Water-in-Water Emulsions by Nanorods. *ACS Macro Lett.* **2016**, *5* (3), 283. https://doi.org/10.1021/acsmacrolett.5b00953.

(45) de Folter, J. W. J.; Hutter, E. M.; Castillo, S. I. R.; Klop, K. E.; Philipse, A. P.; Kegel, W. K. Particle Shape Anisotropy in Pickering Emulsions: Cubes and Peanuts. *Langmuir* **2014**, *30* (4), 955–964. https://doi.org/10.1021/la402427q.

(46) Palange, A. L.; Palomba, R.; Rizzuti, I. F.; Ferreira, M.; Decuzzi, P. Deformable Discoidal Polymeric Nanoconstructs for the Precise Delivery of Therapeutic and Imaging Agents. *Mol. Ther.* **2017**, *25* (7), 1514–1521. https://doi.org/10.1016/j.ymthe.2017.02.012.

(47) Key, J.; Palange, A. L.; Gentile, F.; Aryal, S.; Stigliano, C.; Di Mascolo, D.; De Rosa, E.; Cho, M.; Lee, Y.; Singh, J.; Decuzzi, P. Soft Discoidal Polymeric Nanoconstructs Resist Macrophage Uptake and Enhance Vascular Targeting in Tumors. *ACS Nano* **2015**, *9* (12), 11628–11641. https://doi.org/10.1021/acsnano.5b04866.

(48) Palomba, R.; Palange, A. L.; Rizzuti, I. F.; Ferreira, M.; Cervadoro, A.; Barbato, M. G.; Canale, C.; Decuzzi, P. Modulating Phagocytic Cell Sequestration by Tailoring Nanoconstruct Softness. *ACS Nano* **2018**, *12* (2), 1433–1444. https://doi.org/10.1021/acsnano.7b07797.

(49) Colasuonno, M.; Palange, A. L.; Aid, R.; Ferreira, M.; Mollica, H.; Palomba, R.; Emdin, M.; Del Sette, M.; Chauvierre, C.; Letourneur, D.; Decuzzi, P. Erythrocyte-Inspired Discoidal Polymeric Nanoconstructs Carrying Tissue Plasminogen Activator for the

Enhanced Lysis of Blood Clots. *ACS Nano* **2018**, *12* (12), 12224–12237. https://doi.org/10.1021/acsnano.8b06021.

(50) Binks, B. P.; Horozov, T. S. Colloidal Particles at Liquid Interfaces: An Introduction. In *Colloidal Particles at Liquid Interfaces*; Binks, B. P., Horozov, T. S., Eds.; Cambridge University Press: Cambridge, 2006; pp 1–74. https://doi.org/10.1017/CBO9780511536670.002.

(51) Liu, X.; Shi, S.; Li, Y.; Forth, J.; Wang, D.; Russell, T. P. Liquid Tubule Formation and Stabilization Using Cellulose Nanocrystal Surfactants. *Angew. Chem.* **2017**, *129* (41), 12768–12772. https://doi.org/10.1002/ange.201706839.

(52) Gonzalez Ortiz, D.; Pochat-Bohatier, C.; Cambedouzou, J.; Bechelany, M.; Miele, P. Current Trends in Pickering Emulsions: Particle Morphology and Applications. *Engineering* **2020**, *6* (4), 468–482. https://doi.org/10.1016/j.eng.2019.08.017.

(53) Cook, A. B.; Clemons, T. D. Bottom-Up versus Top-Down Strategies for Morphology Control in Polymer-Based Biomedical Materials. *Adv. NanoBiomed Res.* **2021**, 2100087. https://doi.org/10.1002/anbr.202100087.

(54) Vries, A. de; Gomez, Y. L.; Linden, E. van der; Scholten, E. The Effect of Oil Type on Network Formation by Protein Aggregates into Oleogels. *RSC Adv.* **2017**, *7* (19), 11803–11812. https://doi.org/10.1039/C7RA00396J.

(55) Fujii, S.; Okada, M.; Furuzono, T. Hydroxyapatite Nanoparticles as Stimulus-Responsive Particulate Emulsifiers and Building Block for Porous Materials. *J. Colloid Interface Sci.* **2007**, *315* (1), 287–296. https://doi.org/10.1016/j.jcis.2007.06.071.

(56) Thompson, K. L.; Derry, M. J.; Hatton, F. L.; Armes, S. P. Long-Term Stability of n-Alkane-in-Water Pickering Nanoemulsions: Effect of Aqueous Solubility of Droplet Phase on Ostwald Ripening. *Langmuir* **2018**, *34* (31), 9289–9297. https://doi.org/10.1021/acs.langmuir.8b01835.

(57) Binks, B. P. Particles as Surfactants—Similarities and Differences. *Curr. Opin. Colloid Interface Sci.* **2002**, *7* (1), 21–41. https://doi.org/10.1016/S1359-0294(02)00008-0.

(58) Bon, S. A. F. The Phenomenon of Pickering Stabilization: A Basic Introduction. In *Particle-Stabilized Emulsions and Colloids*; Royal Society of Chemistry, 2014; pp 1–7. https://doi.org/10.1039/9781782620143-00001.

(59) Aveyard, R.; Clint, J. H.; Nees, D.; Paunov, V. N. Compression and Structure of Monolayers of Charged Latex Particles at Air/Water and Octane/Water Interfaces. *Langmuir* **2000**, *16* (4), 1969–1979. https://doi.org/10.1021/la990887g.

(60) Chevalier, Y.; Bolzinger, M.-A. Emulsions Stabilized with Solid Nanoparticles: Pickering Emulsions. *Colloids Surf. Physicochem. Eng. Asp.* **2013**, *439*, 23–34. https://doi.org/10.1016/j.colsurfa.2013.02.054.

(61) Haney, B.; Chen, D.; Cai, L.-H.; Weitz, D.; Ramakrishnan, S. Millimeter-Size Pickering Emulsions Stabilized with Janus Microparticles. *Langmuir* **2019**, *35* (13), 4693–4701. https://doi.org/10.1021/acs.langmuir.9b00058.

(62) Ridel, L.; Bolzinger, M.-A.; Gilon-Delepine, N.; Dugas, P.-Y.; Chevalier, Y. Pickering Emulsions Stabilized by Charged Nanoparticles. *Soft Matter* **2016**, *12* (36), 7564–7576. https://doi.org/10.1039/C6SM01465H.

(63) Bon, S. A. F.; Colver, P. J. Pickering Miniemulsion Polymerization Using Laponite Clay as a Stabilizer. *Langmuir* **2007**, *23* (16), 8316–8322. https://doi.org/10.1021/la701150q.

(64) Trucillo, E.; Bisceglia, B.; Valdrè, G.; Giordano, E.; Reverchon, E.; Maffulli, N.; Porta, G. D. Growth Factor Sustained Delivery from Poly-Lactic-Co-Glycolic Acid Microcarriers and Its Mass Transfer Modeling by Finite Element in a Dynamic and Static Three-Dimensional Environment Bioengineered with Stem Cells. *Biotechnol. Bioeng.* **2019**, *116* (7), 1777–1794. https://doi.org/10.1002/bit.26975.

(65) Morgan, A. R.; Ballard, N.; Rochford, L. A.; Nurumbetov, G.; Skelhon, T. S.; Bon, S. A. F. Understanding the Multiple Orientations of Isolated Superellipsoidal Hematite Particles at the Oil–Water Interface. *Soft Matter* **2012**, *9* (2), 487–491. https://doi.org/10.1039/C2SM26556G.

(66) Tavacoli, J. W.; Katgert, G.; Kim, E. G.; Cates, M. E.; Clegg, P. S. Size Limit for Particle-Stabilized Emulsion Droplets under Gravity. *Phys. Rev. Lett.* **2012**, *108* (26), 268306. https://doi.org/10.1103/PhysRevLett.108.268306.

(67) Kim, E. G.; Stratford, K.; Clegg, P. S.; Cates, M. E. Field-Induced Breakup of Emulsion Droplets Stabilized by Colloidal Particles. *Phys. Rev. E* **2012**, *85* (2), 020403. https://doi.org/10.1103/PhysRevE.85.020403.

(68) Simovic, S.; Prestidge, C. A. Nanoparticle Layers Controlling Drug Release from Emulsions. *Eur. J. Pharm. Biopharm.* **2007**, *67* (1), 39–47. https://doi.org/10.1016/j.ejpb.2007.01.011.